ISSN NO. 2320-5407

Journal homepage: http://www.journalijar.com

INTERNATIONAL JOURNAL OF ADVANCED RESEARCH

RESEARCH ARTICLE

Density Functional Theory (DFT) Studies on Sulfa Dimedine Azo Derivatives as Green Inhibitors for C-Steel in 0.5 M H_3PO_4 Solutions

Hala.M.Hassan[1 *], A.M.Eldesoky [2], R.M.Younis [3] and Wael A. Zordok[4]

1[*]Textile Technology Department, Industrial Education College, Beni-Suef University, Egypt and Chemistry Department, Faculty of Science, Jazan University, KSA.

2Engineering Chemistry Department, High Institute of Engineering & Technology (New Damietta), Egypt and Al-Qunfudah Center for Scientific Research (QCSR), Al-Qunfudah University College, Umm Al-Qura University, KSA.

3Department of Chemistry, Faculty of Science, Mansoura University, Mansour, Egypt and Faculty of Science, Chemistry Department, Tabuk University, KSA.

4Department of Chemistry, Faculty of Science, Zagazig University, Zagazig, Egypt and Department of Chemistry University College of Quanfudha, Umm Al-Qura University, KSA.

Manuscript Info

Manuscript History:

Received: 12 April 2014
Final Accepted: 23 May 2014
Published Online: June 2014

Key words:
DFT Theory, Green Inhibitors, Sulfa Dimedine Azo, C-Steel

Corresponding Author

Hala.M.Hassan

Abstract

The density function theory (DFT) is used to study the structural properties of two sulfa dimedine azo derivatives in aqueous phase in an attempt to understand their inhibition mechanism. The protection efficiencies of these compounds showed a certain relationship to highest occupied molecular orbital (HOMO) energy, Mulliken atomic charges and Fukui indices. Quantum chemical method was also employed to explore the relationship between the inhibitor molecular properties and its protection efficiency. The protection influence of two sulfa dimedine azo derivatives against C-steel corrosion was studied in 0.5 M H_3PO_4 solutions at 25°C. Measurements were conducted under various experimental conditions using Weight loss, potentiodynamic polarization and electrochemical impedance spectroscopy (EIS) techniques. These studies have shown that sulfa dimedine azo derivatives are very good ‘‘green”, inhibitors. Corrosion rates obtained from both Tafel extrapolation and EIS methods are comparable with those recorded using Weight loss method, confirming validation of corrosion rates measured by the latter. The inhibitive action of these sulfa dimedine azo derivatives against C-steel corrosion in 0.5 M H_3PO_4 solutions was discussed in terms of blocking the electrode surface by adsorption of the molecules through the active centers contained in their structures following Temkin adsorption isotherm.

Copy Right, IJAR, 2014,. All rights reserved.

INTRODUCTION

Phosphoric acid is a medium-strong acid, but it still shows strong corrosiveness on ferrous alloy [1]. Phosphoric acid is widely used in surface treatment of steel such as chemical and electrolytic polishing, chemical coloring, chemical and electrolytic etching, removal of oxide film, phosphating, passivating, and surface cleaning. Using inhibitors is an effective method for corrosion to control the corrosion of metals. Inhibitors are compounds that control corrosion processes of metals. Many studies on inhibitors have been carried out [2-8], among them nitrogen containing inhibitor is one of the focuses of the studies [8-24]. Bentiss et al. [11], El Azhar et al. [16] and Elkadi et al. [20] have investigated many nitrogen-containing inhibitors for the corrosion inhibition of steel in HCl and H_2SO_4, their studies show that nitrogen-containing organic inhibitor acts as a strong inhibitor for steel in HCl, compared with H_2SO_4. Triazole and triazole-type compounds containing nitrogen, sulphur and heterocycle on the

corrosion inhibition of metal in acidic media have attracted more attention because of their excellent corrosion inhibition performance [25-28]. The researches by Fouda et al. showed that some 4-phenylthiazole derivatives could inhibit the corrosion of 304L stainless steel in hydrochloric acid solution, but the inhibition effect was not very excellent [29]. Wang et al. also investigated the effect of some mercapto-triazole derivatives synthesized containing different hetero atoms and substituents in the organic structures on the corrosion and hydrogen permeation of mild steel in hydrochloric acid solution and their results revealed that all the mercapto-triazole derivatives performed excellently as corrosion inhibitors [30]. Especially, some N-and S-containing triazole derivatives are environmentally friendly corrosion inhibitors compared with some commercial acid corrosion inhibitors which are highly toxic, such as chromate and nitrite [31].

The sulfa dimedine azo derivatives which are the object of the present investigation are non-toxic, cheap and environmental friendly. They contain reactive centers like N atoms containing lone pairs of electrons and aromatic rings with delocalize π-electron systems which can aid their adsorption onto metal surfaces. Furthermore, they have high molecular weights and are likely to effectively cover more surface area (due to adsorption) of the metal thus preventing corrosion from taking place.

In this work, the density function theory (DFT) is used to study the structural properties of two sulfa dimedine azo derivatives in aqueous phase in an attempt to understand their inhibition mechanism. The protection efficiencies of these compounds showed a certain relationship to the highest occupied molecular orbital (E_{HOMO}) and the lowest unoccupied molecular orbital (E_{LUMO}), the energy difference (ΔE) between E_{HOMO} and E_{LUMO}. It was also the purpose of the present work to discuss the corrosion inhibition of C-steel in acidic medium using two sulfa dimedine azo derivatives and to propose a suitable mechanism for the inhibition using the potentiodynamic polarization and ac impedance spectroscopy methods.
The names, chemical and molecular structures of the investigated derivatives are shown in Table (1) [32].

2. Computational Details

Density functional theory (DFT) was used to compute of the effect some sulfa dimedine azo compounds on the degree of inhibition for the corrosion rate theoretically and detect the exact structure of these compounds also show the stable compound which can be used as inhibitor more than others. The effect of substitution was investigated theoretically and the excited state for all compounds was investigated by applying UV calculations to determine the different types of electronic transition which can be occurred on these compounds with different substituent. The Frontier molecular orbitals were studied for its important role in the electric and optical properties, as well as in UV-Vis. Spectra and chemical reactions. Such computational characterization reduces time consuming experiments for biomedical and pharmaceutical studies of the drugs and its complexes. Profiles of the optimal set and geometry of these complexes were simulated by applying the GAUSSIAN 98W package of programs [33] at B3LYP/Cep-31G [34] level of theory.

3. Experimental Details

3.1. Materials Preparation

The chemical composition wt % of C-steel was as follows: 0.200 C, 0.350 Mn, 0.024 P, 0.003 Si, 0.023 and the remainder Fe. Seven pieces of C- steel were cut into 2 x 2 x 0.2 cm .The specimens were polished with a series of emery papers of different grit size up to 1200, degreased in acetone [35], rinsed with double distilled water and finally dried between two filter papers and then weighed. After that these specimens were immersed in 100 ml solution of H_3PO_4 without and with different concentrations of the studied inhibitors for 3 hours at temperature range from 25 ºC to 55 ºC, at the end of the tests the specimens were taken out, washed, dried and weighed again.Then the average weight loss calculated at certain time of each specimen was taken.

3.2 Electrochemical Techniques

For Electrochemical measurements (potentiodynamic polarization and EIS techniques) the cell used was a conventional three electrodes Pyrex glass with a platinum foil counter electrode and a standard calomel electrode (SCE) as reference. The working electrode was C-steel electrode, which cut from C-steel sheets with thickness 0.1 cm. The electrode was of dimensions 1 cm x 1 cm and was weld from one side to a copper wire used for electric connection. The sample was embedded in a glass tube using epoxy resin [36]. The cell was filled with constant quantity of the test solution (100 ml). The electrode potential was allowed to stabilize for 30 min before starting the measurements. The potentiodynamic current-potential curves were recorded by changing the electrode potential automatically from - 500 to + 500 mV with a scan rate of 5 mV s^{-1}. Experiments for electrochemical impedance

spectroscopy (EIS) measurements were conducted in the frequency range of 100 kHz to 10 mHz at open circuit potential (OCP). The amplitude was 5 mV. The electrochemical measurements were carried out using Potentiostat / Galvanostat / Zera analyzer (Gamry PCI 300/4). This includes Gamry framework system based on the ESA400, and a personal computer with DC 105 software for potentiodynamic polarization, EIS 300 software for EIS measurements. Echem Analyst 5.58 software was used for plotting, graphing and fitting data.

4. Results and Discussion

4.1. Theoretical (Computational) Study

The geometric parameters and energies were computed by density functional theory at the B3LYP/Cep-31G level of theory, using the GAUSSIAN 98W package of the programs, on geometries that were optimized at Cep-31G basis set. The high basis set was chosen to detect the energies at a highly accurate level. The atomic charges were computed using the natural atomic orbital populations. The B3LYP is the keyword for the hybrid functional [37], which is a linear combination of the gradient functional proposed by Becke [38] and Lee, Yang and Parr [39], together with the Hartree-Fock local exchange function [40].

Table (1): The Names, Chemical and Molecular Structures of the Investigated Derivatives

Cpd. No.	Name	Structure	Molecular Weight & Chemical Formula
(I)	Sulfa Dimedine Azomethine Salisaldehyde	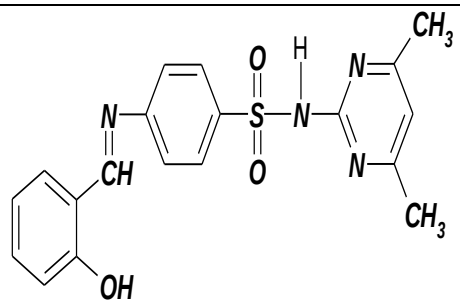	382.0, $C_{19}H_{18}N_4O_3S$
(II)	Sulfa Dimedine Azo Salisaldehyde	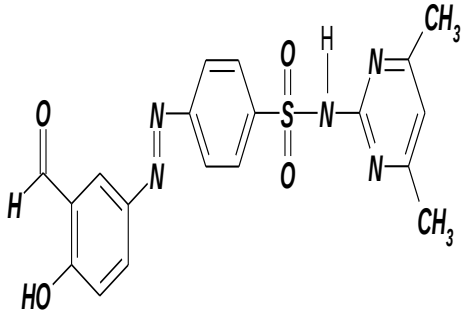	395.0, $C_{19}H_{17}N_5O_3S$

4.1.1. Structural Parameters and Model of Sulfa Compounds

I- Sulfa Dimedine Azomethine Salisaldehyde

The activity of sulfa compounds is mainly determined by its fine structure, the sulfa dimedine azomethine salisaldhyde has many characteristic structural features. The molecule is a highly sterically-hindered, there are three aromatic rings. The molecule is non planer, there are two plans one occupied by central aromatic ring and other plane occupied by the two terminal aromatic rings and also, the two plans are perpendicular respect to each other. The bond length C1-N2 is 1.263Å, C3-N6 is 1.264 Å, there is a double bond characters C and N atoms, whereas N19-C20 is double bond 1.348Å [41]. Detailed analysis of corresponding bond lengths in various sulfa molecules was given elsewhere. All distances and angles between the atoms of the sulfa compound system are given in Table (2). The S10-O11 and S10-O12 bond lengths are 1.439 Å and 1.438 Å respectively, the C26-O27 bond length is 1.356 Å

The molecule is a highly sterically-hindered, the sulfa dimedine azomethine salisaldhyde compound occupied two plans they are perpendicular to each other. The terminal diazine ring and phenyl ring are out of plane of central aromatic ring the dihedral angle N9S10C13C18, 56.94˚ and N9S10C13C14, -120.33˚, so the diazine ring is axially oriented from the ring. Also the terminal phenyl ring lying out of plane of the molecule. This observation

is supported by the values of calculated dihedral angles: C20N19C16C15, 128.21˚, and C20N19C16C17, -54.59˚, where the values are neither zero nor 180˚. Fig.(1), shows the optimized geometrical structure of sulfa dimedine azomethine salisaldhyde compound, the dihedral angles C5N6C3N9 is 177.94 and N2C3N9S10 is 10.14˚ also, N6C3N9S10, -167.98˚ and C3N9S10O11 is 160.88˚ which confirms that the S10 and N6 lying in the opposite direction. The dihedral angles C16N19C20C21 is -28.61˚ and C20N19C16C17 is -54.59˚ also, C20N19C16C15, 128.21˚ and N19C20C21C26 is -3.63˚, C20C21C26O27 is - 5.00˚ which confirms that The C20N19 bond lying in the same plane of C26O27 bond and the phenyl ring is not lying in the same plane of the central aromatic ring.

Table (2) gives the optimized geometry of sulfa dimedine azomethine salisaldhyde as obtained from B3LYP/Cep-31G calculations. These data are drowning to give the optimized geometry of molecule. The value of bond angle C3N9S10 is 125.69˚, O11S10O12 is 124.49˚, N9S10C13 is 99.25˚ and C16N19C20 is 122.17˚ reflects on sp^2 hybridization of N19, the same result is obtained with C20, the bond angle N19C20N21 is 134.55˚. The values of bond distances are compared nicely with that obtained from X-ray data [42]. Comparisons of the performance of different DFT methods allow outlining the main trends of these theoretical approaches which are necessary to better understand the properties and reaction mechanisms of sulfa dimedine azomethine salisaldhyde compound. However, till now, no attempt has been made to analyze the application of various DFT methods and different basis sets for accurate calculations of structure of sulfa dimedine azomethine salisaldhyde [43- 46].

The S atom is bonded strongly with surrounded two oxygen atoms, nitrogen and carbon atom, Also the charge accumulated on S10 (1.229), O11 (-0.602) and O12 (-0.596). The charge accumulated in N9 (-0.430), N19 (-0.254) and N2 (-0.357), N6 (-0.361). The presence of OH group effect on the charge spreading overall sulfa compound, the charge on O27 (-0.366) and C26 (0.238). The energy of this compound is -238.37159173 au and highly dipole 10.898D.

II- Sulfa Dimedine Azo Salisaldehyde

The molecule is non planer, there are two plans one occupied by two aromatic rings around the azo-group and other plane occupied by the terminal aromatic diazine ring and also, the two plans are perpendicular respect to each other. The bond length C1-N2 is 1.263Å, C5-N4 is 1.265 Å, there is a double bond characters C and N atoms, whereas N20-N21 is double bond 1.248Å. All distances and angles between the atoms of the sulfa compound system are given in Table (3). The S11-O12 and S11-O13 bond lengths are 1.439 Å, the C25-O29 bond length is 1.361 Å and the bond length C28-O31 of aldhyde is 1.209 with double bond character.

The molecule is a highly sterically-hindered, the Sulfa dimedine azo salisaldehyde compound occupied two plans they are perpendicular to each other. This result can be confirmed from the values of the dihedral angle N2C3N9S11, -14.06˚ and N4C3N9S11, 167.22˚, where the values are neither zero nor 180˚, so the diazine ring is axially oriented from the ring and then out of plane occupied by other two aromatic rings around azo group. Also the two aromatic rings around the azo group lying in the same plane. This observation is supported by the values of calculated dihedral angles: C17N20n21C22, 179.32˚, and N20N21C22C23, 179.74˚, O29C25C24C23 is -179.99˚. Fig.(2), shows the optimized geometrical structure of Sulfa dimedine azo salisaldehyde compound, the dihedral angles C23C24C28O31 is 0.17˚ and O29C25C24C23 is -179.99˚ which confirms that the O31 of aldhyde group and O29 of phenol not lying in the same direction.

Table (3) gives the optimized geometry of sulfa dimedine azo salisaldehyde as obtained from B3LYP/Cep-31G calculations. These data are drowning to give the optimized geometry of molecule. The value of bond angle C3N9S11 is 125.56˚, O12S11O13 is 124.28˚, N9S11C14 is 101.18˚ and C17N20N21 is 117.70˚ and N20N21C22 is 118.44˚ reflects on sp^2 hybridization of N20, the same result is obtained with N21, also, the same result can be observed on the C28, the bond angle C24C28O31 is 125.96˚.

The S atom is bonded strongly with surrounded two oxygen atoms, nitrogen and carbon atom, Also the charge accumulated on S11 (1.228), O12 (-0.599) and O13 (-0.597). The charge accumulated in N9 (-0.429), also the charge accumulated on two nitrogen atoms of azo group N20 is (-0.126) and N21 is (-0.09). The charge on N2 (-0.362), N4 (-0.359). The presence of OH and CHO groups effect on the charge spreading overall sulfa compound, the charge on O29 (-0.343), C25 (0.245) and O31 (-0.313), C28 (0.265), C24 (-0.059). The energy of this compound is -265.204872223 au and not highly dipole 7.34D which result from the presence of CHO group adjacent to OH group.

4.1.2. Frontier Molecular Orbitals

The frontier molecular orbitals play also an important role in the electric and optical properties, as well as in UV-Vis. Spectra and chemical reactions [47]. Fig. 3 shows the distributions and energy levels of HOMO and LUMO orbitals computed for the all sulfa compounds. For sulfa dimedine azomethine salisaldhyde compound the values of the energy of HOMO and LUMO are given in Table (4), the difference between HOMO and LUMO is

0.10502 and for sulfa dimedine azo salisaldehyde compound the values of HOMO and LUMO are given in Table (4), the difference between HOMO and LUMO is 0.06548, also the values of $HOMO^{-1}$, $HOMO^{-2}$, $LUMO^{+1}$ and $LUMO^{+2}$ are given in Table (4)

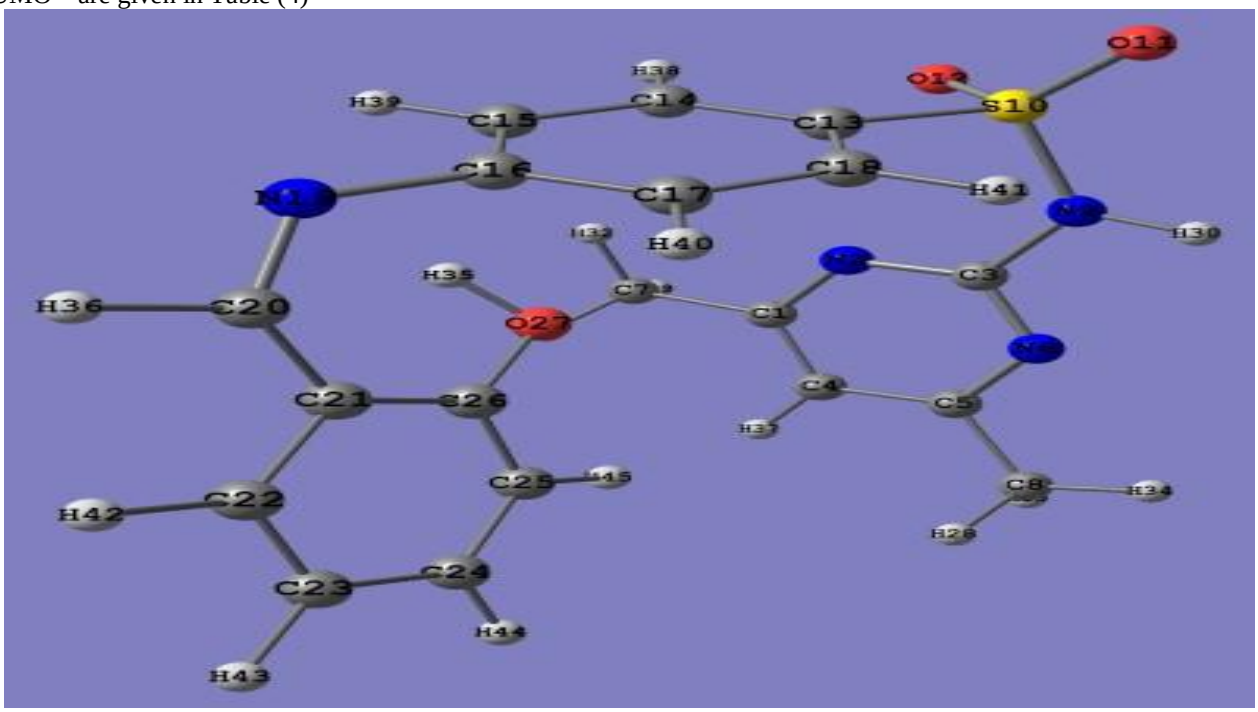

Fig. (1): The Optimized Geometrical Structure of Sulfa Dimedine Azomethine Salisaldhyde Compound by Using B3LYP/Cep-31G

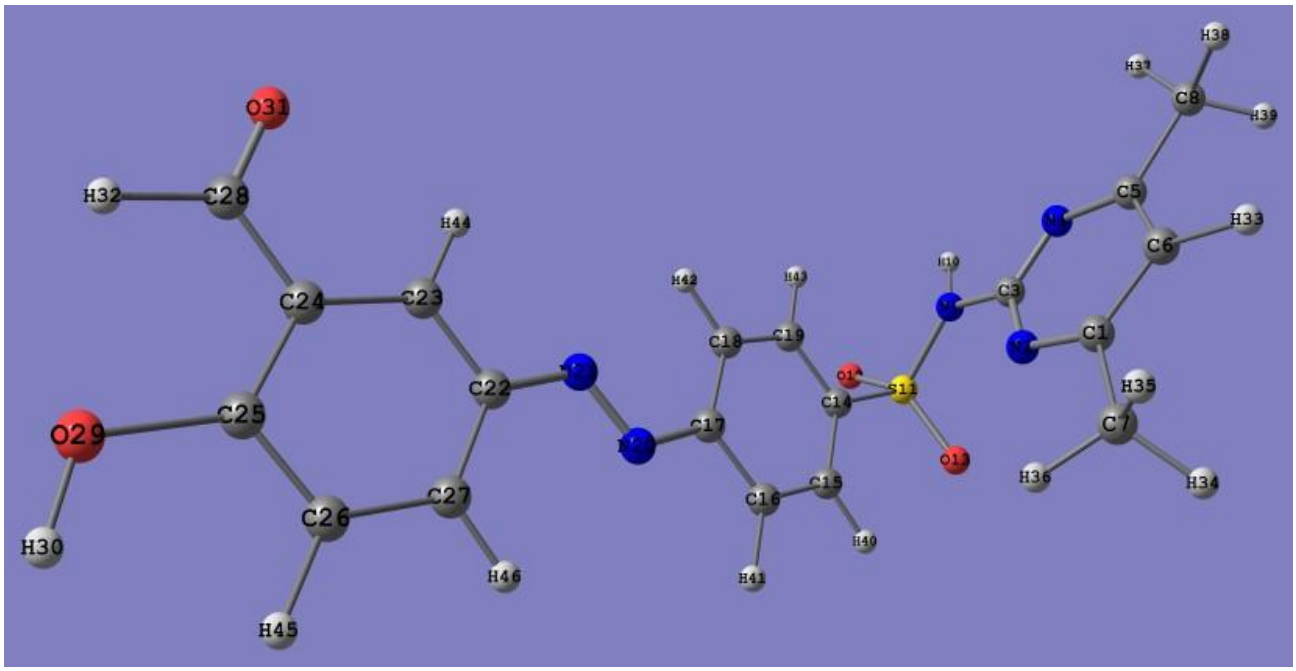

Fig. (2): Optimized Geometrical Structure of Sulfa Dimedine Azo Salisaldehyde Compound by Using B3LYP/Cep-31G

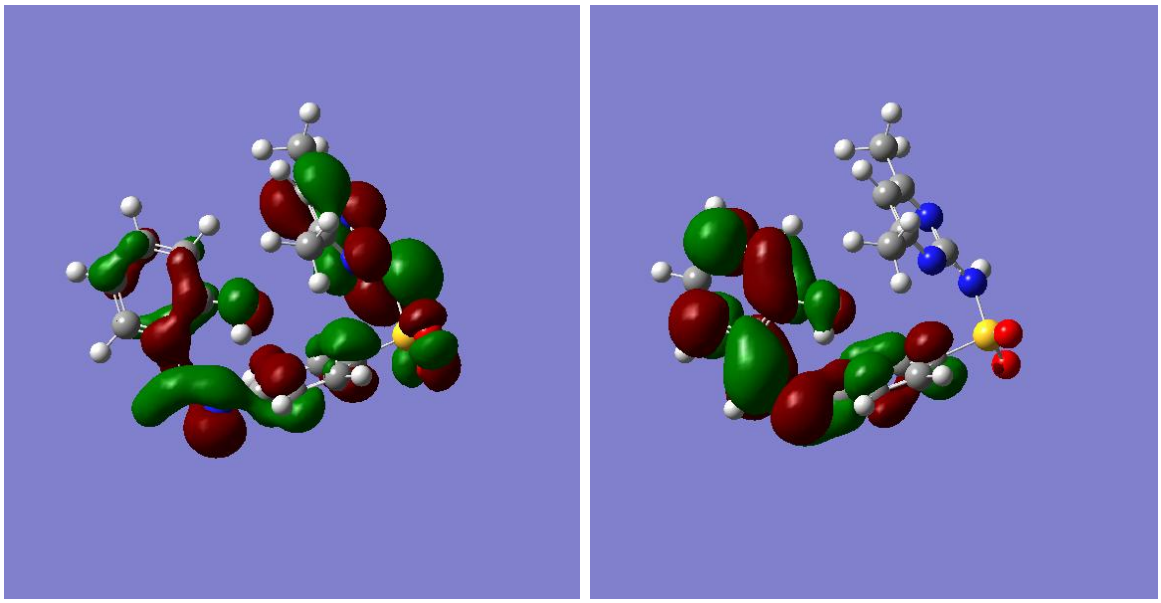

(I) HOMO LUMO

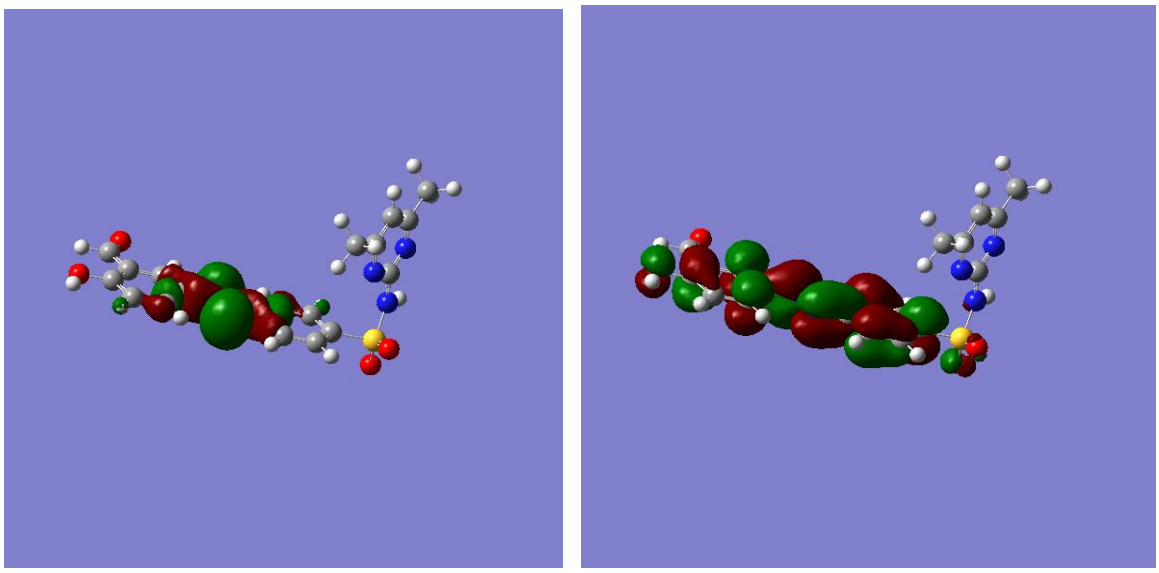

(II) HOMO LUMO

Fig. (3); Molecular Orbital Surfaces and Energy Levels of (I) Sulfa Dimedine Azomethine Salisaldhyde and (II) Sulfa Dimedine Azo Salisaldehyde Compound by Using B3LYP/Cep-31G

Table (2): Equilibrium Geometric Parameters Bond Lengths (Å), Bond Angles (˚), Dihedral Angles (˚) and Charge Density of Sulfa Dimedine Azomethine Salisaldhyde Compound by Using DFT/B3LYP/Cep-31G.

Bond length (Å)							
C5-C8	1.505	C3-N9	1.347	C15-C16	1.342	C21-C22	1.351
C5-N6	1.264	N9-S10	1.638	C16-C17	1.342	C22-C23	1.341
C3-N6	1.264	S10-O11	1.439	C17-C18	1.342	C23-C24	1.338
N2-C3	1.264	S10-O12	1.438	C13-C18	1.347	C24-C25	1.339
C1-N2	1.263	S10-C13	1.745	C16-N19	1.346	C25-C26	1.345
C1-C4	1.341	C13-C14	1.347	N19-C20	1.348	C26-O27	1.356
C1-C7	1.504	C14-C15	1.343	C20-C21	1.350		

Bond angle (˚)							
N6C5C8	117.17	N6C3N9	117.06	O11S10C13	100.41	C16N19C20	122.17
C4C5C8	122.86	C3N9S10	125.69	C18C13S10	119.51	N19C20C21	134.55
N2C1C7	116.78	N9S10C13	99.25	C14C13S10	122.11	C20C21C22	115.52
C3N6C5	120.14	O11S10O12	124.49	C14C13C18	118.33	C20C21C26	126.93
N2C3N6	122.49	N9S10O11	111.86	C15C16C17	119.71	C21C26O27	123.58
C1N2C3	120.66	N9S10O12	112.56	C17C16N19	120.54	C21C26C25	119.55
N2C3N9	120.43	O12S10C13	103.56	C15C16N19	119.69	C25C26O27	116.79

Dihedral angles (˚)					
C5N6C3N9	177.94	C18C13S10O11	-57.48	C20N19C16C15	128.21
N6C3N9S10	-167.98	C14C13S10O11	125.45	C16N19C20C21	-28.61
N2C3N9S10	10.14	C14C13S10O12	-4.29	N19C20C21C26	-3.63
C3N9S10O11	160.88	C14C18C13S10	-175.35	C20C21C26O27	-5.00
C3N9S10O12	-53.29	C15C14C13S10	175.59	C22C21C26O27	-6.69
C18C13S10O12	172.99	C20N19C16C17	-54.59	N9S10C13C19	56.94

Charges							
C1	0.287	C8	-0.206	C15	-0.101	C22	0.001
N2	-0.357	N9	-0.430	C16	0.209	C23	-0.054
C3	0.463	S10	1.229	C17	-0.092	C24	0.016
C4	-0.234	O11	-0.602	C18	0.019	C25	-0.099
C5	0.278	O12	-0.596	N19	-0.254	C26	0.238
N6	-0.361	C13	-0.084	C20	0.107	O27	-0.366
C7	-0.204	C14	0.025	C21	-0.042		
Total energy/au				**-238.37159173**			
Total dipole moment/D				**10.898**			

Table (3): Equilibrium Geometric Parameters Bond Lengths (Å), Bond Angles (˚), Dihedral Angles (˚) and Charge Density of Sulfa Dimedine Azo Salisaldehyde Compound by Using DFT/B3LYP/Cep-31G.

Bond Length (Å)							
C1-C7	1.504	C5-C8	1.505	C16-C17	1.345	C22-C23	1.346
C1-N2	1.263	N9-S11	1.636	C17-C18	1.346	C23-C24	1.345
N2-C3	1.264	S11-O13	1.439	C18-C19	1.343	C24-C25	1.347
C3-N4	1.264	S11-O12	1.439	C14-C19	1.345	C25-C26	1.344
C5-N4	1.265	S11-C14	1.743	C17-N20	1.266	C26-C27	1.342
C5-C6	1.342	C14-C15	1.345	N20-N21	1.248	C25-O29	1.361
C1-C6	1.341	C14-C16	1.343	N21-C22	1.266	C28-O31	1.209
Bond Angle (˚)							
N2C1C7	116.69	C3N9S11	125.56	C17C18C19	120.86	C23C24C28	119.08
C6C1C7	123.67	N9S11C14	101.18	C16C17C18	117.88	C24C28O31	125.96
C1C6C5	117.18	N9S11O13	112.29	C15C16C17	121.27	C25C24C28	119.73
C6C5C8	123.23	N9S11O12	111.76	C14C15C16	120.86	C24C25O29	122.65
C6C5N4	119.89	O12S11O13	124.28	C16C17N20	116.54	C24C25C26	117.26
C8C5N4	116.87	C14S11O13	103.26	C18C17N20	125.58	C26C25O29	120.09
C3N4C5	120.19	C14S11O12	99.91	C17N20N21	117.70	C25C26C27	121.97
N2C3N4	122.56	C15C14S11	121.89	N20N21C22	118.44	C22C27C26	120.49
N4C3N9	116.99	C19C14S11	120.22	N21C22C23	116.42		
C1N2C3	120.53	C15C14C19	117.89	C22C23C24	120.99		
N2C3N9	120.44	C14C19C18	121.24	C23C24C25	121.19		

Dihedral Angles (˚)					
C3N2C1C3	179.58	O13S11C14C19	164.15	C23C24C28O31	0.17
C8C5N4C3	-179.89	O13S11C14C15	-16.39	O29C25C24C23	-179.99
N4C3N9S11	167.22	O12S11C14C19	-66.92	C17N20N21C22	179.32
N2C3N9S11	-14.06	O12S11C14C15	112.55	N20N21C22C23	179.74
N9S11C14C15	-132.74	N9S11C14C19	47.80		

Charges							
C1	0.283	C8	-0.206	C16	-0.068	C23	-0.023
N2	-0.362	N9	-0.429	C17	0.179	C24	-0.059
C3	0.463	S11	1.228	C18	-0.071	C25	0.245
N4	-0.359	O12	-0.599	C19	0.003	C26	-0.105
C5	0.280	O13	-0.597	N20	-0.126	C27	-0.019
C6	-0.233	C14	-0.656	N21	-0.09	C28	0.265
C7	-0.206	C15	0.008	C22	0.124	O29	-0.343
						O31	-0.313
Total energy/au				**-265.204872223**			
Total dipole moment/D				**7.34**			

Table (4): Values of Energy (eV) of HOMO and LUMO for the (I) Sulfa Dimedine Azomethine Salisaldhyde and (II) Sulfa Dimedine Azo Salisaldehyde Compound by Using B3LYP/Cep-31G.

	(I)	**(II)**
$LUMO^{+2}$	-0.14096	-0.14713
$LUMO^{+1}$	-0.14889	-0.1869
LUMO	**-0.20035**	**-0.21273**
HOMO	**-0.30537**	**-0.27821**
$HOMO^{-1}$	-0.31135	-0.29958
$HOMO^{-2}$	-0.31618	-0.3047
ΔE= HOMO - LUMO	**0.10502**	**0.06548**

4.2. Weight Loss Measurements

Weight loss of C-steel was determined at several time intervals in the absence and presence of different concentrations of sulfa dimedine azo derivatives (I-II). Figure (4) shows the weight loss-time curves for C-steel corrosion at different concentrations of inhibitor (I) at 25 °C. Similar curve was obtained for other compound (not shown). The curves obtained show that the weight loss of C-steel in presence of inhibitor is lower than free acid and decreases with increasing inhibitors concentrations [48]. This means that these compounds act as inhibitors for C-steel in 0.5 M H_3PO_4 solutions. The degree of surface coverage (θ) and the inhibition efficiency (% IE) were calculated using the following equation:

$$\%IE = \theta \times 100 = [1-(W_{inh}/W_{free})] \times 100 \quad (1)$$

Where W_{inh} and W_{free} are the weight losses per unit area in presence and absence of the inhibitor, respectively. Values of % IE are listed in Table (5). The values of inhibition efficiency increases with increasing inhibitor concentration. This behavior could be attributed to the increase of the surface area covered by the adsorbed molecules of inhibitors with the increase of its concentration. At the same concentration of inhibitors, the order of inhibition efficiency was found to be as follows: Compound (II) > Compound (I).

Table (5): Inhibition Efficiency (% IE) at Different Concentrations of Inhibitors for the Corrosion of C-Steel after 90 min Immersion in 0.5 M H_3PO_4 at 25 ºC.

Conc., M	% IE	
	(I)	(II)
$1 \chi 10^{-6}$	27.2	33.8
$5 \chi 10^{-6}$	36.0	52.7
$10 \chi 10^{-6}$	51.1	59.1
$15 \chi 10^{-6}$	59.5	63.3
$20 \chi 10^{-6}$	64.5	69.2
$25 \chi 10^{-6}$	66.2	71.7

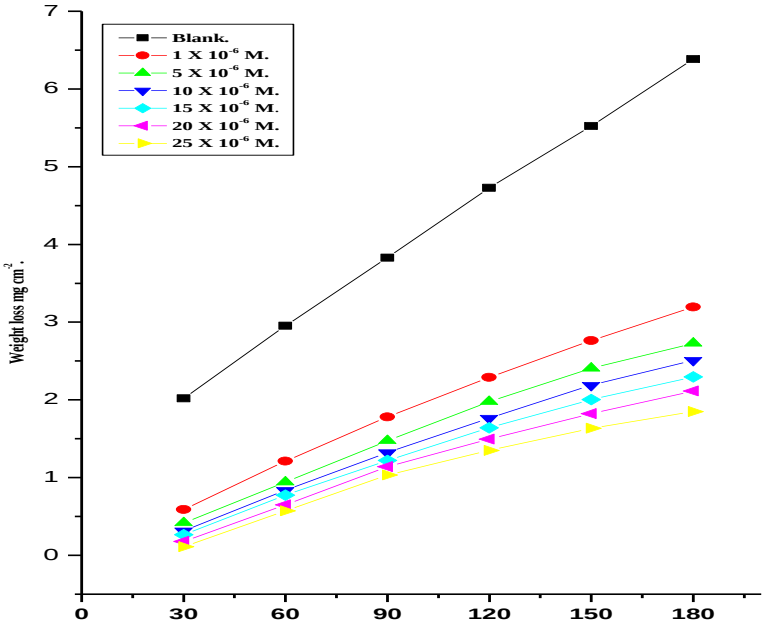

Fig. (4): Weight Loss-Time Curves for the Dissolution of C-Steel in the Absence and Presence of Different Concentrations of Inhibitor (I) in 0.5 M H_3PO_4 at 25˚C.

4.2.1. Adsorption Isotherm

Sulfa dimedine azo derivatives inhibit corrosion of C-steel by adsorbing onto the metal surface in acid solution. Basic information on the interaction between the inhibitor and the metal can be provided by the adsorption isotherm. The values of surface coverage (θ) corresponding to different concentrations of the inhibitor have been used to determine the adsorption isotherm. The variation of surface coverage (θ) determined by weight loss with the logarithm of the inhibitor (I) concentration with log C, at different temperatures are represented in Figure (5). Similar curve were obtained for other inhibitor (not shown). The linear relationships of θ vs.log C depicted in Fig. 5 with correlation coefficient nearly equal to 1.0 ($R^2 > 0.9$) suggest that the adsorption of sulfa dimedine azo derivatives from 0.5 M H_3PO_4 solution on C-steel obeys the Temkin adsorption isotherm. According to this isotherm the surface coverage is related to inhibitor concentration by:

$$K_{ads}C = \exp(-2a\theta) \quad (2)$$

Where "a" is the molecular interaction parameter and K_{ads} is the equilibrium constant of the adsorption process. The free energy of adsorption $\Delta G°_{ads}$ was calculated from the following equation [49]:

$$\Delta G°_{ads} = - RT \ln (55.5\ K) \quad (3)$$

Where 55.5 is the concentration of water in solution in mol l^{-1}, R is the universal gas constant and T is the absolute temperature. By applying the following the equation $\Delta G°_{ads} = \Delta H°_{ads} - T\ \Delta S°_{ads}$ and plot $\Delta G°_{ads}$ versus T linear relationships with slope equal ($- \Delta S°_{ads}$) and intercept of ($\Delta H°_{ads}$) were obtained. The data were collected in Table 6. From data in Table 6 we can conclude that:

- Negative sign of $\Delta G°_{ads}$ indicates that the adsorption of sulfa dimedine azo derivatives on C-steel surface is proceeding spontaneously [50, 51].
- Generally, values $\Delta G°_{ads}$ of up to – 20 kJ mol^{-1} are consistent with physisorption , while those around - 40 $kJmol^{-1}$ or higher are associated with chemisorptions as a result of the sharing or transfer of electrons from organic molecules to the metal surface to form a coordinate bond . From the obtained values of $\Delta G°_{ads}$ it was found the existence of comprehensive adsorption (physisorption and chemisorption) [52], that is to say, since the adsorption heat approached the general chemical reaction heat, the chemical adsorption occurs.
- Negative sign of $\Delta H°_{ads}$ indicates that the process of adsorption is exothermic [53].
- Positive sign of $\Delta S°_{ads}$ arises from substitutional process, which can be attributed to the increase in the solvent entropy .This lead to an increase in disorder due to the fact that more water molecules can desorbed from the metal surface by one inhibitor.

Table (6): Thermodynamic Parameters for the Adsorption of Sulfa Dimedine Azo derivatives on C-Steel Surface in 0.5 M H_3PO_4 at Different Iemperatures.

Temp. °C	$K_{ads}x10^{-6}$ M^{-1}	$-\Delta G°_{ads}$ kJ mol^{-1}	$-\Delta H°_{ads}$ kJ mol^{-1}	$\Delta S°_{ads}$ J mol^{-1} K^{-1}
(I)				
25	1.12	43.9	28.0	57.1
35	0.71	44.7		
45	0.55	45.4		
55	0.43	47.0		
(II)				
25	3.53	46.0	27.5	67.9
35	2.61	47.9		
45	2.10	48.9		
55	1.22	49.5		

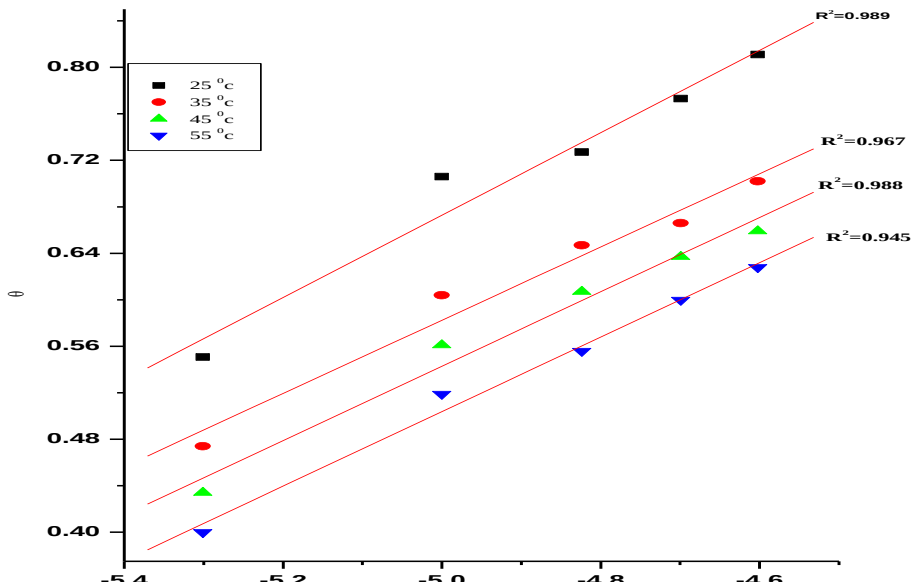

Fig. (5): Temkin Adsorption Isotherm for C-steel in 0.5 M H_3PO_4 in the Presence of Different Concentrations of Inhibitor (I) at Different Temperatures.

4.2.2. Effect of Temperature

The effect of temperature on both corrosion inhibition of C-steel in 0.5 M H_3PO_4 solution in the absence and presence of different concentrations of sulfa dimedine azo derivatives at different temperatures ranging from 25 to 55 °C was investigated. The apparent activation energies (E*a) for the corrosion reaction of C-steel in 0.5 M H_3PO_4 solution in the absence and presence of different concentrations of sulfa dimedine azo derivatives were calculated from Arrhenius type equation [54]:

$$\text{Log } k_{corr} = \log A - E^*_a / (2.303RT) \quad (5)$$

Where A is the Arrhenius pre-exponential factor. A plot of log k_{corr} versus 1/T gave straight lines as shown in Figure (6). The enthalpy of activation (ΔH*) and the entropy of activation (ΔS*) were obtained by applying the transition-state equation [55]:

$$\log(k_{corr}/T) = [\log(R/Nh) + (\Delta S^*/ 2.303R) - (\Delta H^*/ 2.303RT)] \quad (6)$$

A plot of log (k_{corr}/T) versus 1/T gave straight lines as shown in Figure (7). With a slope of (-ΔH*/ 2.303R) and intercept of [log(R/Nh) + (ΔS*/ 2.303R)] from which the values of ΔH* and ΔS* were calculated, respectively. All estimated thermodynamic-kinetic parameters were tabulated in Table (7). The obtained data in Table (7) can be interpreted as follows:

- The presence of inhibitors increases the activation energies of C- steel indicating strong adsorption of the inhibitor molecules on the metal surface and the presence of these additives induces energy barrier for the corrosion reaction and this barrier increases with increasing the inhibitor concentrations.
- Higher activation energy means lower reaction rate and the opposite is true. The increase in activation energy with inhibitor concentration is often interpreted by physical adsorption with the formation of an adsorptive film of an electrostatic character.
- Values of ΔH* are positive. This indicates that the corrosion process is an endothermic one.
- The entropy of activation (ΔS*) in the absence and presence of inhibitor has negative values, this indicates that the activated complex in the rate determining step represents an association rather than dissociation, meaning that, a decrease in disordering takes place on going from reactants to the activated complex [55].

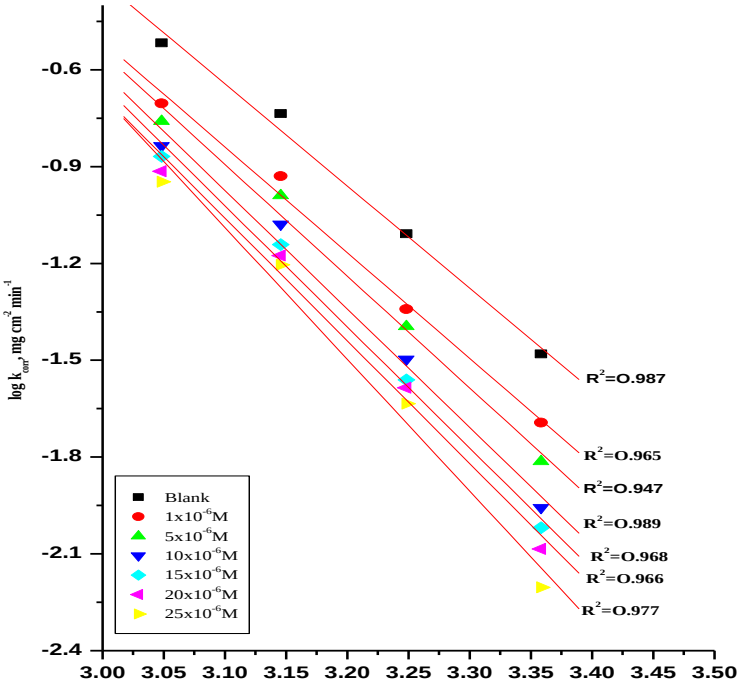

Fig. (6): Arrhenius Plots for C-Dissolution in 0.5 M H_3PO_4 in the Absence and Presence of Different Concentrations of Inhibitor (I).

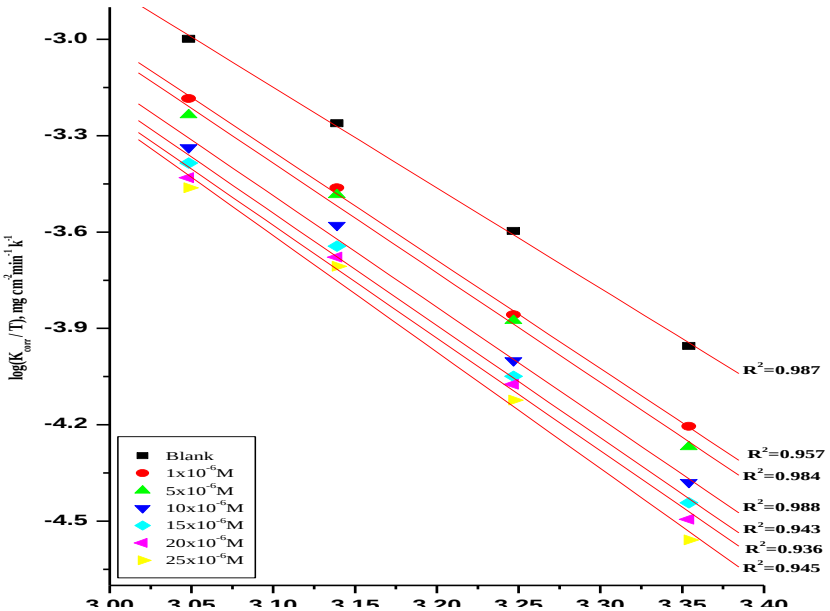

Fig. (7): Transition State Plots for C-Dissolution in 0.5 M H_3PO_4 in the Absence and Presence of Different Concentrations of Inhibitor (I).

Table (7): Thermodynamic activation parameters for the dissolution of C-steel in 0.5 M H_3PO_4 in the absence and presence of different concentrations of investigated inhibitors.

Inhibitor	Conc., M	E_a^* kJ mol^{-1}	ΔH^* kJ mol^{-1}	$-\Delta S^*$ J mol^{-1} K^{-1}
Blank	------	61.6	59.9	70.5
(I)	1 X 10^{-6}	62.4	62.7	67.3
	5 X 10^{-6}	61.9	63.2	66.8
	10 X 10^{-6}	65.3	64.3	64.7
	15 X 10^{-6}	65.7	66.0	60.5
	20 X 10^{-6}	66.7	66.5	60.0
	25 X 10^{-6}	67.6	67.3	59.1
(II)	1 X 10^{-6}	60.8	63.6	66.1
	5 X 10^{-6}	62.9	64.3	65.0
	10 X 10^{-6}	67.5	65.0	64.3
	15 X 10^{-6}	68.0	66.3	60.4
	20 X 10^{-6}	68.2	65.9	59.7
	25 X 10^{-6}	71.40	68.2	55.4

4.3. Electrochemical Techniques

4.3.1 Potentiodynamic Polarization Technique

The kinetics of anodic and cathodic reactions occurring on C-steel electrodes in 0.5 M H_3PO_4 in the absence and presence of different concentrations of sulfa dimedine azo derivatives was investigated using potentiodynamic polarization technique. Figure (8) shows the polarization curves in the absence and presence of inhibitor (I) at 25°C. Similar curve was obtained for other inhibitor (not shown). The numerical values of the variation of the corrosion current density (i_{corr}), the corrosion potential (E_{corr}), Tafel slopes (β_a & β_c), degree of surface coverage (θ) and the inhibition efficiency (% IE) were calculated from equation 7 are given in Table (8).

$$\% \text{ IE} = [1 - (i_{corr} / i^o_{corr})] \times 100 \qquad (7)$$

Where i^o_{corr} and i_{corr} correspond to uninhibited and inhibited corrosion current densities, respectively.

The results indicate that:

1. The cathodic and anodic curves obtained exhibit Tafel–type behavior. Additional of sulfa dimedine azo derivatives increased both the anodic and cathodic overvoltages
2. The corrosion current density (i_{corr}) decreases with increasing the concentrations of the sulfa dimedine azo derivatives which indicates that these compounds acts as inhibitors, and the degree of inhibition depends on the concentrations of inhibitor
3. The slopes of the anodic and cathodic Tafel lines (β_a & β_c) were slightly changed on increasing the concentrations of inhibitors . This indicates that there is no change of the mechanism of the inhibition in presence and absence of inhibitors .The sulfa dimedine azo derivatives are mixed – type inhibitors [57], but the cathode is more polarize than the anode when an external current was applied. The higher values of Tafel slopes can be attributed to surface kinetic process rather the diffusion-controlled process.
4. The order of inhibition efficiency of all inhibitors at different concentrations as given by polarization measurements are listed in Table (8). The results are in good agreement with that obtained from weight–loss measurements.

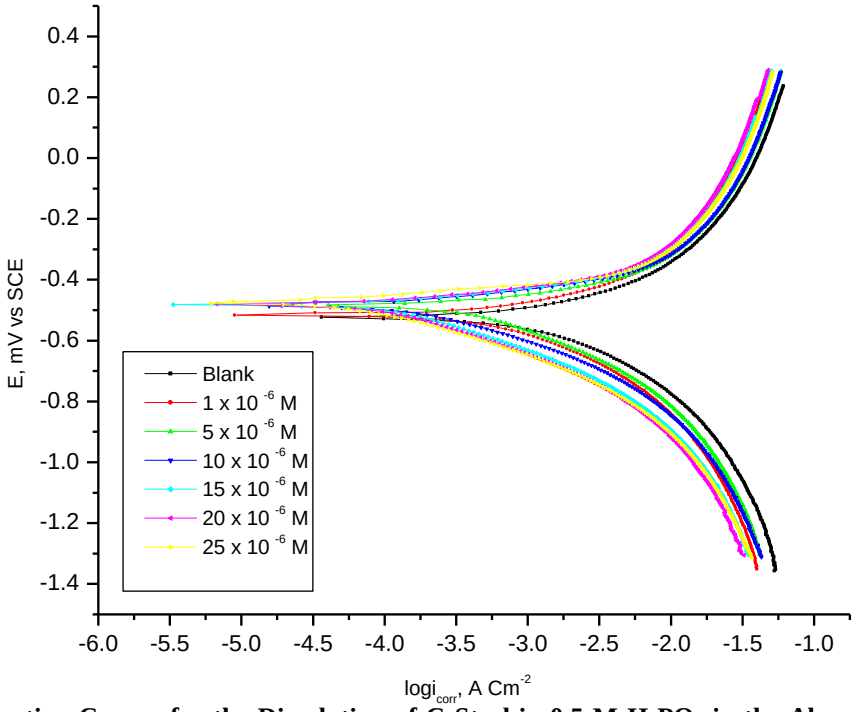

Fig. (8): Polarization Curves for the Dissolution of C-Steel in 0.5 M H_3PO_4 in the Absence and Presence of Different Concentrations of Inhibitor (I) at 25 °C.

Table (8): Electrochemical Kinetic Parameters Obtained from Potentiodynamic Polarization Technique for the Corrosion of C-Steel in 0.5 M H_3PO_4 at Different Concentrations of Investigated Inhibitors at 25 °C.

Inh.	Conc M	$-E_{corr}$, mV,vs SCE	i_{corr} mA cm^{-2}	β_c mV dec^{-1}	β_a mV dec^{-1}	θ	% IE
Blank	---------	525	5.53	763	649	-------	-------
(I)	1 X 10^{-6}	514	3.80	711	587	0.312	31.2
	5 X 10^{-6}	517	3.44	679	564	0.377	37.7
	10 X 10^{-6}	503	2.59	642	527	0.531	53.1
	15 X 10^{-6}	508	1.81	560	478	0.672	67.2
	20 X 10^{-6}	504	1.40	525	439	0.746	74.6
	25 X 10^{-6}	503	1.20	484	403	0.783	78.3
(II)	1 X 10^{-6}	511	3.39	683	561	0.386	38.6
	5 X 10^{-6}	494	2.49	617	497	0.549	54.9
	10 X 10^{-6}	479	1.03	479	399	0.813	81.3
	15 X 10^{-6}	472	0.74	448	359	0.866	86.6
	20 X 10^{-6}	485	0.66	424	364	0.880	88.0
	25 X 10^{-6}	489	0.49	411	352	0.911	91.1

4.3.2. Electrochemical Impedance Spectroscopy Technique (EIS)

Electrochemical impedance spectroscopy was used to characterized the corrosion inhibition and adsorbed behavior of C-steel electrode in 0.5 M H_3PO_4 containing various concentrations of sulfa dimedine azo derivatives Figure (9) shows the typical EIS diagram obtained in 0.5 M H_3PO_4 with and without inhibitor at frequency ranging from 100 kHz to 0.1 Hz.

The equivalent circuit model which describes the metal / electrolyte interface of the present corroding system is shown as insert in Figure (10), where Rs, R_{ct} and CPE refer to solution resistance, charge transfer resistance and constant phase element representing the double layer capacitance (C_{dl}) of the interface, respectively. The charge transfer resistance (R_{ct}) is calculated from the difference in impedance at lower and higher frequencies [58]. The double layer capacitance (C_{dl}) and the frequency at which the imaginary component of impedance is maximal ($-Z_{max}$) are found as the follow [59]**:**

$$\mathbf{C_{dl} = 1 / (2\,\pi\, fmax\, R_{ct})} \qquad \mathbf{(8)}$$

The inhibition efficiencies obtained from the EIS measurements are calculated from the relation [60]:

$$\mathbf{\%\ IE = [1 - (R_{ct} / R`_{ct})]\ x100} \qquad \mathbf{(9)}$$

Where R_{ct} and $R`_{ct}$ are the transfer resistance without and with the inhibitor, respectively.

Figure (9) the impedance diagrams consists of one large capacitive loop. In fact, the presence of inhibitors enhances the value of R_{ct} in acidic solution indicating a charge-transfer process mainly controlling the corrosion of C-steel. The impedance parameters derived from this investigation are given in Table (9) these parameters can be concluded as follows:

- R_{ct} increased by increasing the concentrations of sulfa dimedine azo derivatives giving consequently a decrease in the corrosion rate.
- C_{dl} values decreased with increasing inhibitor concentration this is due to the gradual replacement of water molecules in the double layer by the adsorbed inhibitor molecules which form on adherent film on the metal surface and leads to decrease in the local dielectric constant of the metal solution interface [61].
- i_{corr} values decrease significantly in the presence of these additives and the % IE is greatly improved. The order of reduction in i_{corr} exactly correlates with that obtained from potentiodynamic polarization studies.
- The inhibition achieved by these inhibitors decreases in the following sequences Compound (II) > Compound (I)

It can be concluded that the inhibition efficiency found from weight loss, polarization curves and electrochemical impedance spectroscopy measurements are in good agreement.

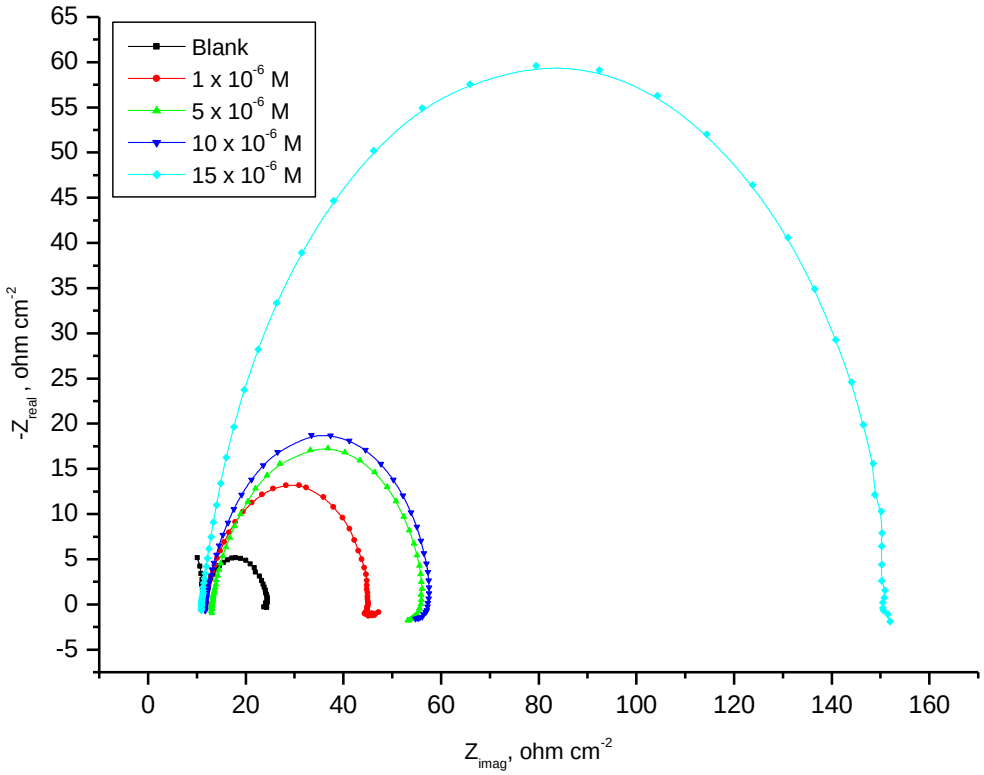

Fig. (9): Nyquist Plots for C-Steel in 0.5 M H_3PO_4 Solution in the Absence and Presence of Different Concentrations of Inhibitor (I) at 25 °C.

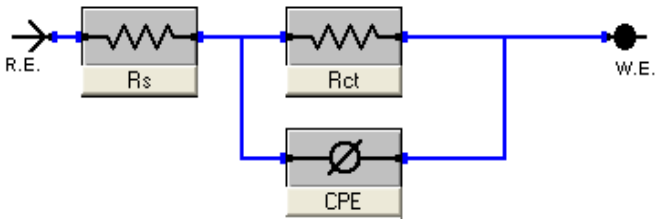

Fig. (10): Electrical Equivalent Circuit Used to Fit the Impedance Data for C-Steel in 0.5 M H_3PO_4 Solution.

Table (9): Electrochemical Kinetic Parameters Obtained from EIS Technique for the Corrosion C-Steel in 0.5M H_3PO_4 at Different Concentrations of Investigated Inhibitors at 25°C

Inhibitor	Conc., µM	C_{dl}x10^{-3}, µF cm^{-2}	R_{ct}, Ω cm^2	θ	% IE
Blank	-------	122.9	12.75	----	----
(I)	1 X 10^{-6}	95.7	26.96	0.528	52.8
	5 X 10^{-6}	81.9	27.88	0.542	54.2
	10 X 10^{-6}	51.0	30.68	0.585	58.5
	15 X 10^{-6}	47.0	33.26	0.616	61.6
(II)	1 X 10^{-6}	54.9	28.91	0.558	55.8
	5 X 10^{-6}	48.9	33.01	0.613	61.3
	10 X 10^{-6}	56.1	34.90	0.634	63.4
	15 X 10^{-6}	58.0	84.96	0.849	84.9

4.4. Mechanism of Corrosion Inhibition

The essential effect of these sulfa dimedine azo compounds as corrosion inhibitors is due to the presence of free electron pairs in the nitrogen, oxygen and sulfur atoms, d π-electrons on the aromatic rings, molecular size, heat of hydrogenation, mode of interaction with the metal surface and formation of metallic complexes.

It is well known that C- steel has co-ordination affinity toward N, O and S bearing ligand. Hence, adsorption on C-steel can be attributed to co-ordination through hetero-atoms and π-electrons of aromatic rings [62]. In all investigated sulfa dimedine azo derivatives, there are unshared electron pairs on N, O and S, capable of forming σ-bond with C- steel. Further, the double bonds in the molecule allow back donation of metal d-electron to the π^*-orbital. Another striking feature for high inhibition performance of all studied sulfa dimedine azo derivatives is the presence of S-atom. The presence of S-atom in the inhibitor structure makes the formation of dπ-dπ bond resulting from overlap of 3d-electrons from C-steel the 3d vacant orbital of S-atom possible, which enhances the adsorption of the compounds on the metal surface. Also the lower solubility of sulfur compounds and the greater polarizability of sulfur atoms increase the inhibition efficiency of these compounds.

Compound (II) is the most efficient one, which is due to the presence of 1S, 5 N, and 3 O atoms in its structure and high molecular weight , but compound (I) comes after compound (II) in inhibition efficiency. This is due to the smaller number of nitrogen atoms (4 N atoms) in its structure and lower molecular weight.

The bond gap energy ΔE increases from (II to I). This fact explains the decreasing inhibition efficiency in this order (II > I), as shown in Table (4) and Fig (3) show the optimized structures of the two investigated compounds. So, the calculated energy gaps show reasonably good correlation with the efficiency of corrosion inhibition. Table (4) also indicates that compound (II) possesses the lowest total energy that means that compound (II) adsorption occurs easily and is favored by the highest softness. The HOMO and LUMO electronic density distributions of these molecules were plotted in Fig (3). For the HOMO of the studied compounds that the benzene ring, N-atoms and O-atom have a large electron density.

5. References

[1] Y. Jianguo, W.Lin, V.Otieno-Alego, D.P.Schweinsberg, Corros. Sci., 37(1995).
[2] E.E. Foad, El. Sherbini, Mater. Chem. Phys. 60 (1999) 286.
[3] G. Lewis, Corros. Sci. 22 (1982) 579.
[4] G. Schmitt, Br. Corros. J. 19 (1984) 165.
[5] M. Bartos, N. Hackerman, J. Electrochem. Soc. 139 (1992) 3429.
[6] S.L. Granese, Corrosion 44 (1988) 322.
[7] F. Zucchi, G. Trabanelli, G. Brunoro, Corros. Sci. 33 (1992) 1135.
[8] P. Chatterjee, M.K. Benerjee, K.P. Mukherjee, Indian J. Technol. 29(1991) 191.
[9] M. Elachouri, M.S. Hajji, S. Kertit, E.M. Essassi, M. Salem, R.Coudert, Corros. Sci. 37 (1995) 381.
[10] B. Mernari, H. Elattari, M. Traisnel, F. Bentiss, M. Larenée, Corros.Sci. 40 (1998) 391.
[11] F. Bentiss, M. Traisnel, N. Chaibi, B. Mernari, H. Vezin, M. Lagrenée,Corros. Sci. 44 (2002) 2271.
[12] L. Elkadi, B. Mernari, M. Traisnel, F. Bentiss, M. Lagrenée, Corros.Sci. 42 (2000) 703.
[13] A. Elkanouni, S. Kertit, A. Ben Bachir, Bull. Electrochem. 12 (1996)517.
[14] R. Walker, Corros. Sci. 31 (1975) 97.
[15] S. Kertit, B. Hammouti, Appl. Surf. Sci. 93 (1996) 59.
[16] M. El Azhar, B. Mernari, M. Traisnel, F. Bentiss, M. Lagrenée, Corros. Sci. 43 (2001) 2229.
[17] L.B. Tang, G.N. Mu, G.H. Liu, Corros. Sci. 45 (2003) 2251.
[18] D.Q. Zhang, L.X. Gao, G.D. Zhou, J. Appl. Electrochem. 33(2003)361.
[19] A.B. Tadros, B.A. Abdenaby, J. Electroanal. Chem. 246 (1988) 433.
[20] L. Elkadi, B. Mernari, M. Traisnel, F. Bentiss, M. Lagrenée, Corros.Sci. 42 (2000) 703.
[21] R.J. Chin, K. Nobe, J. Electrochem. Soc. 118 (1971) 545.
[22] R. Agrawal, T.K.G. Namboodhiri, J. Appl. Electrochem. 22 (1972)383.
[23] N. Eldakar, K. Nobe, Corrosion 32 (1976) 128.
[24] F. Bentiss, M. Traisnel, M. Lagrenée, Corros. Sci. 42 (2000) 127.
[25] W.Qafsaoui, H.Takenouti, Corros. Sci. 52(2010) 3667-3677.
[26] M.Finsgar, I.Milosev, , Corros. Sci. 52(2010) 2737-2749.
[27] M.L.Zheludkevich, K.A.Yasakau, S.K.Poznyak, M.G.S.Ferreira, Corros.Sci.,47 (2005) 3368-3383.
[28] F.Bentiss, M.Traisnel, L.Gengembre, M.Lagrenee, Appl. Surface Sci. 161(2000) 194-202.
[29] I A.S. Fouda, A.S. Ellithy, Corros. Sci. 51(2009) 868-875.
[30] H.L.Wang, R.B.Liu, J.Xin, Corros.Sci. 46(2004) 2455-2466.
[31] F.Bentiss, M.Lagrenee, M.Traisnel, J.C.Hornez, Corros. Sci. 41(1999) 789-803.
[32] I. Sheikhshoaie, M. Hossein, Mashhadizadeh, and S. Saeid-Nia,J .Coordination Chemistry. 57(5) (2004)417.
[33] **Gaussian 98**, Revision A.6, M. J. Frisch, G. W. Trucks, H. B. Schlegel, G. E. Scuseria, M.A.Robb, J.R.Cheeseman, V.G. Zakrzewski, J.A. Montgomery, Jr.,R.E.Stratman J.C.Burant, S.Dapprich, J.M.Millam, A.D.Daniels, K.N. Kudin, M.C. Strain, O. Farkas, J. Tomasi, V. Barone, M. Cossi, R. Cammi, B.Mennucci, C. Pomelli, C. Adamo, S.Clifford, J. Ochterski, G. A. Petersson, P. Y. Ayala, Q. Cui, K. Morokuma, D. K.Malick, A.D.Rabuck, K. Raghavachari, J.B. Foresman, J.Cioslowski, J.V.Ortiz, B.B.Stefanov, G.Liu, A.Liashenko, P.Piskorz, I. Komaromi, R.Gomperts,R. L. Martin, D. J. Fox, T. Keith, M. A. Al-Laham, C. Y. Peng, A. Nanayakkara, C. Gonzalez, M. Challacombe, P. M. W. Gill, B. Johnson, W. Chen, M. W. Wong, J. L.Andres, C. Gonzalez, M. Head-Gordon, E. S. Replogle, and J. A. Pople, Gaussian, Inc., Pittsburgh PA, (1998)
[34] W. J. Stevens, M. Krauss, H. Bosch and P. G. Jasien, Can. J. Chem. 70 (1992)612.
[35] K.F. Bonhoeffer and K.E. Heascer, Z. Phys. Chem., NE8 (1956) 390.
[36] A.S. Fouda, S.S. El-Kaabi and A. K. Mohamed, Corros. Prevention Control, 164(1990) 164.
[37] W. Kohn, L. J. Sham, Phys. Rev A 140(1965)1133.
[38] A. D. Becke, Phys. Rev. A 38(1988)3098.
[39] C. Lee, W. Yang, R. G. Parr, Phys. Rev B (1988)37.
[40] R. L. Flurry Jr., Molecular Orbital Theory of Bonding in Organic Molecules, Marcel Dekker, New York, 1968.
[41] I. Turel, L. Golic, P. Bukovec and M. Gubina, Journal of Inorganic Biochemistry 71(1998)53.
[42] I. Turel, P. Bukovec, M. Quiros, Int. J. Pharm. 152 (1997) 59.
[43] Yue Yang, Hongwei Gao, Spectrochemica Acta part A 85(2012) 303-309
[44] S.Sagdinc and S. Bayari, Journal of Molecular Structure 691(2004)107-113
[45] A. Yoshida, R. Moroi, Anal. Sci. 7(1991)351
[46] S.Sagdinc and S. Bayari, Journal of Molecular Structure (THEOCHEM) 668(2004)93-99
[47] I. Fleming Frontier Orbitals and Organic Chemical Reactions, Wiley, London, 1976.
[48] M.Sahin, S.Bilgic and H . Ylmaz, Apl. Surf. Sci .195 (2002) 1

[49] F. Bentiss, M. Traisnel, N. Chaibi, B. Mernari, H. Vezin, M. Lagrenée,Corros. Sci. 44 (2002) 2271
[50] A. A. El- Awady, B. Abd El-Nabey and S. G. Aziz, Electrochem. Soc. 139 (1992) 2149
[51] S.S. Abd El-Rehim, H.H. Hassan and M.A. Amin, Mater. Chem. Phys. 70 (2001) 64
[52] Li X. and Mu G.," Tween-40 , Appl. Surf. Sci., 252 (2005) 1254.
[53] L. Tang, G. Murad and G. Liu, Corros. Sci. 45 (2003) 2251.
[54] I. N. Putilova, S. A. Balzin and V. P. Barannik, Metallic Corrosion Inhibitors, Pergamomon Press , New York (1960) 31.
[55] X. Li And L. Tang, Mater .Chem. Phys. 90 (2005) 286
[56] C. Jeyaprabha, S. Sathiyanarayanan and G. Venkatachari, Appl. Surf. Sci., 246 (2005) 108
[57] M. A. Amin, S. S. Abd El-Rehim, E. E. F. El-Sherbini and R. S. Bayoumi, Elactrochim, Acta, 52 (2007) 3588
[58] T. Tsuru, S. Haruyama and B. B. Gijutsu, J. Jpn. Soc . Corros.Eng. 27(1978)
[59] J. Ross.Macdonald, Impedance, Spectroscopy, Jon Wiley and Sons, (1987)
[60] S. S. Abd El-Rehim, A. M. Magdy and K. F. Khaled, J. Appl.Elactrochem., 29(1999) 593-599
[61] A. S. Fouda , F. El- Taib . Heakal. And M. S. Radwan, J. Appl . Electrochem, 39 (2009) 391-402
[62] I. Ahmad, R. Prasad and M. A. Quraishi, Corros. Sci., 52 (2010) 3033.